Supporting Information for Bathymetric influences on Antarctic ice-shelf melt rates

D. N. Goldberg[1], T. A. Smith[2], S. H. K. Narayanan[3], P. Heimbach[2,4,5], M. Morlighem[6]

[1]School of Geosciences, University of Edinburgh, Edinburgh, United Kingdom

[2]Oden Institute for Computational Engineering and Sciences, The University of Texas at Austin, Austin, Texas

[3]Mathematics and Computer Science Division, Argonne National Laboratory

[4]Jackson School of Geosciences, The University of Texas at Austin, Austin, Texas

[5]Institute for Geophysics, The University of Texas at Austin, Austin, Texas

[6]University of California Irvine, Department of Earth System Science, Irvine, California

Contents of this file

Additional Supporting Information (Files uploaded separately)

Corresponding author: D N Goldberg, School of GeoSciences, University of Edinburgh. (dan.goldberg@ed.ac.uk)

Introduction

The supplemental text gives an overview of changes made to the MITgcm to support this work. Supplemental text S1 details modification of the implicit free surface code to avoid differentiating through the linear solver. Supplemental text S2 describes Resilient Adjoints, a mechanism to save the state of the adjoint model for the purpose of restarting across multiple HPC batch runs.

Supplemental Figure S1 gives a schematic aiding the explanation of Resilient Adjoints. Supplemental Figure S2 shows the perturbed stream functions for the four regions of bathymetric perturbation in the "ISOMIP-bump" experiment detailed in Section 3 of the main text.

Output datasets S1 and S2 are generated from the output of the MITgcm ocean model and its adjoint, in NETCDF format; there are two separate data files, one for our idealised ISOMIP-bump Experiment and one for our realistic Dotson-Crosson ice shelves experiment. The data was created in July and August of 2019.

Processing methodology is described in our main text.

Text S1. Modifications to the MITgcm adjoint

The MITgcm, and in particular a configuration using the `SHELFICE` physics package for an Antarctic ice shelf, has been differentiated algorithmically (Heimbach & Losch, 2012), and so no additional modifications were required for applications to ice sheet-ocean interactions. However, there are technical issues in using bathymetry as a control variable. For instance, fluid fractions at grid cell faces (see Section 2 of main text) are based on the minimum fraction of adjacent cells, leading to potential non-differentiability. We adopt the approach of Losch & Heimbach (2007) of "smoothing" the min/max functions, but we note that this feature has not been used outside of bathymetric sensitivity studies.

Another computational challenge in treating bathymetry as a control variable lies with the implicit solve for the free surface at each time step (Marshall et al., 1997). The model solves the linear system $\mathbf{A}\eta = \mathbf{b}$ for η, where η is the free surface at the next time step, and $\mathbf{b}$ is a field arising from the baroclinic step of the model. $\mathbf{A}$ is a linear, self-adjoint operator on η and the propagation of sensitivity from η to b can be calculated analytically:

$$\delta^*\mathbf{b} = \mathbf{A}^{-1}\delta^*\eta, \tag{1}$$

where $\delta^*\eta$ is the *adjoint sensitivity* of η and likewise for $\mathbf{b}$. This formulation is standard in the MITgcm for adjoint based sensitivity analyses of any control variable except for fluid depth. However, the operator $\mathbf{A}$ depends on ocean column depth, which in the present study is a control variable, and therefore the backward-propagation of sensitivities from η to $\mathbf{A}$ must be considered as well. Losch & Heimbach (2007) dealt with this issue by allowing the AD tool to differentiate the linear solver code; however, as it is an iterative solver, this approach requires storing intermediate variables at each solver iteration during every time step of the forward model, which hinders performance and does not scale well to

high dimensional problems. Losch & Heimbach (2007) recommend, but do not implement, using the approach of Giles et al. (2002), which augments Eqn. (1) with

$$\delta^* \mathbf{A} = -\delta^* \mathbf{b} \; \eta^T. \tag{2}$$

In this work we implement this approach, obviating the need for the AD tool to differentiate the implicit solver.

Text S2. Resilient Adjoints

Simulation of large models requires the use of high performance computing (HPC), generally with defined job time limits. For instance, standard batches on the ARCHER supercomputer have a walltime limit of 24 hours (there is a special queue for jobs that take up to 48 hours, but there are fewer resources available and generally longer wait times for this queue). Additionally, imposed time limits aside, longer computational jobs increase the risk of network or server errors leading to crashes. The MITgcm has a restart capability allowing to circumvent these limits: the "state" of the model is periodically saved to file, and new jobs can begin from this time stamp by reading the saved state. To restart the adjoint model, simulations must save both the forward and adjoint states – a capability referred to as *resilient adjoints*. A similar capability was previously implemented with TAF as *the Divided Adjoint* (DIVA).

Here we provide an overview of resilient adjoints, a strategy that enhances the default checkpointing scheme used by OpenAD. Checkpointing approaches store the state of the primal (forward) computation and reduce the amount of memory that is required to compute adjoints. By default, OpenAD uses binomial checkpointing for the time-stepping loop (Griewank & Walther, 2000). Consider a computation consisting of l timesteps, with

c the number of checkpoints that can be stored. Figure S2 (top) illustrates binomial checkpointing for $l = 10$ and $c = 3$.

A two-level checkpointing approach can build upon this approach by converting the time stepping loop into a loop nest containing l_2 outer iterations and l_1 inner iterations where $l = l_2 \times l_1$ (Aupy et al., 2014). The inner loop uses binomial checkpointing as before; the outer loop uses periodic checkpointing. The left part of Figure S2 (bottom) illustrates two level checkpointing for $l_2 = 5$, $l_1 = 10$ and $c_1 = 3$. The resilient adjoints capability enhances two level checkpointing by storing to disk the adjoint state computed at the end of each outer level iteration. To restart a computation at the granularity of an l_2 timestep then, only the stored l_2 state checkpoints and the last adjoint checkpoint, if any, are required.

Data Set S1.

This dataset contains model output from the ISOMIP-bump experiment of Section 3 of the paper, in netcdf format. The file contains the following dimensions and fields:

Dimensions:

- *lon*: longitude, size 50
- *lat*: latitude, size 100
- *depth*: vertical elevation, size 30

Fields:

- *double lon(lon)*; longitude values
- *double lat(lat)*; latitude values
- *double depth(depth)*; depth values (m)
- *double temp(depth, lat)*; zonally averaged temperature (deg C)
- *double melt(lon, lat)*; ice shelf melt rates (kg/m2/s)
- *double topo(lon, lat)*; ice shelf topography (m) 2
- *double strmfunc(lon, lat)*; depth averaged stream function (Sv)
- *double melt_pert_R1(lon, lat)*; region 1 perturbed stream function
- *double melt_pert_R2(lon, lat)*; region 2 perturbed stream function
- *double melt_pert_R3(lon, lat)*; region 3 perturbed stream function
- *double melt_pert_R4(lon, lat)*; region 4 perturbed stream function
- *double sensitivity(lon, lat)*; bathymetric adjoint sensitivity (kg/my)

Data Set S2.

This dataset contains relevant model output from the Dotson-Crosson experiment of Section 4 of the paper, in netcdf format. The file contains the following dimensions and fields:

Dimensions:

- *X*: longitude, size 50
- *Y*: latitude, size 100
- *depth*: vertical elevation, size 30
- *n_front*: index of points across Dotson ice front
- *time*: time in months (1 to 12)

Fields:

- *double X(X)*; X values (m)
- *double Y(Y)*; Y values (m)
- *double depth(depth)*; depth values (m)
- *double x_front(n_front)*; x values along dotson front (m)
- *double y_front(n_front)*; y values along dotson front (m)
- *double month(time)*; month values
- *double millan_bathy(X,Y)* ; processed bathymetry used in ocean model (m)
- *double millan_draft(X,Y)*; processed ice topo used in ocean model (m)
- *double strmfunc(X,Y)*; depth averaged stream function (Sv)
- *double outflow(n_front,depth)*; outflow (cm/s)
- *double avgmelt(X,Y)*; melt rate (kg/m/yr)

- *double melt_sensitivity(X,Y)*; bathymetric adjoint sensitivity of melt rates (kg/m-y)
- *double vaf_sensitivity(X,Y)*; bathymetric adjoint sensitivity of VAF (nondim)
- *double melt(time)*; area averaged melt (kg/yr)
- *double delta_star_hfacc(time)*; RMS of cell center thickness adjoint sensitivities (kg/yr-m)
- *double delta_star_hfacs(time)*; RMS of cell south face thickness adjoint sensitivities (kg/yr-m)
- *double delta_star_hfacw(time)*; RMS of cell west face thickness adjoint sensitivities (kg/yr-m)

References

Aupy, G., Herrmann, J., Hovland, P., & Robert, Y. (2014, 04). Optimal multistage algorithm for adjoint computation. *SIAM Journal on Scientific Computing*, *38*. doi: 10.1137/15M1019222

Giles, M. B., Corliss, G., Faure, C., Griewank, A., Hascoët, L., & Naumann, U. (2002). On the iterative solution of adjoint equations. In *Automatic differentiation of algorithms: From simulation to optimization* (pp. 145–151). New York, NY: Springer New York. doi: 10.1007/978-1-4613-0075-5-16

Griewank, A., & Walther, A. (2000, March). Algorithm 799: Revolve: An implementation of checkpointing for the reverse or adjoint mode of computational differentiation. *ACM Trans. Math. Softw.*, *26*(1), 19–45. Retrieved from `http://doi.acm.org/10.1145/347837.347846` doi: 10.1145/347837.347846

Heimbach, P., & Losch, M. (2012). Adjoint sensitivities of sub-ice shelf melt rates to

ocean circulation under Pine Island Ice Shelf, West Antarctica. *Annals of Glaciol.*, *54*, 59–69. doi: 10.3189/2012/AoG60A025

Losch, M., & Heimbach, P. (2007). Adjoint sensitivity of an ocean general circulation model to bottom topography. *Journal of Physical Oceanography*, *37*(2), 377-393. Retrieved from `https://doi.org/10.1175/JPO3017.1` doi: 10.1175/JPO3017.1

Marshall, J., Hill, C., Perelman, L., & Adcroft, A. (1997). Hydrostatic, quasi-hydrostatic, and nonhydrostatic ocean modeling. *Journal of Geophysical Research: Oceans*, *102*(C3), 5733–5752. Retrieved from `http://dx.doi.org/10.1029/96JC02776` doi: 10.1029/96JC02776

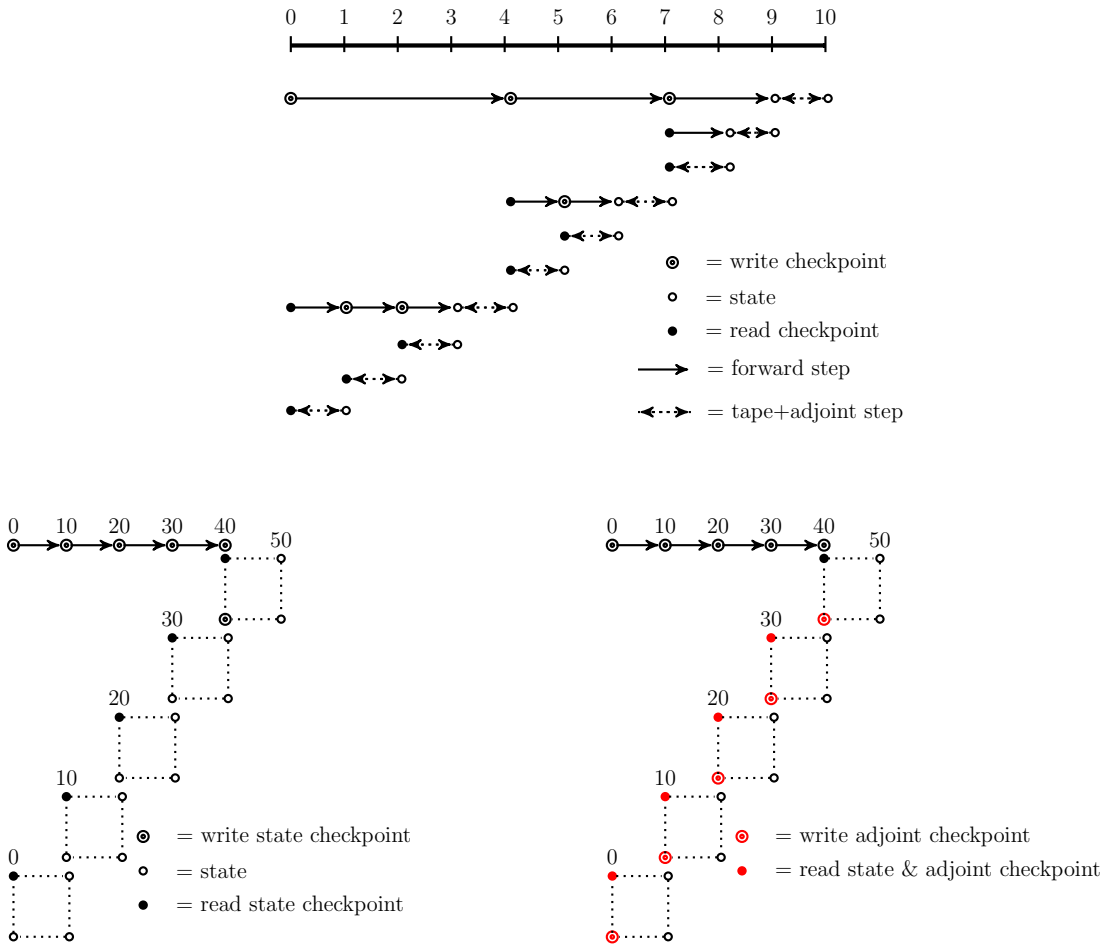

Figure S1. Top: Binomial checkpointing schedule for $l = 10$ time steps and $c = 3$ checkpoints. Bottom Left: Two level checkpointing schedule for $l = 50$ with $(l_2 = 5)$ outer level iterations and $(l_1 = 10)$ inner level iterations. Periodic checkpointing is used in the outer level and binomial checkpointing shown by the dashed box is used at the inner level. Bottom Right: Enhanced two level checkpointing schedule with support for resilient adjoints through the writing and reading of the adjoint state at the outer level.

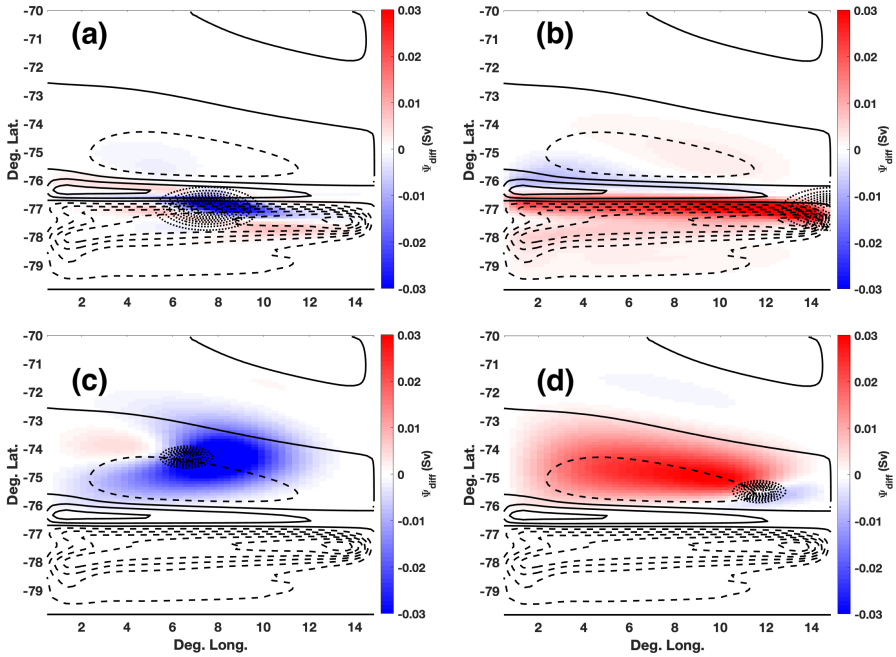

Figure S2. Perturbed beds (dotted contours) and corresponding perturbed barotropic stream functions (shading) in different regions of high sensitivity in Fig. 3 of the main text. (a) through (d) correspond to finite perturbations in locations (1) through (4) in Fig. 3(a) of the main text, respectively. Bathymetric peturbations plotted with δR=10 (Eqn. 3 of the main text) and 1m isolines. Isolines of unperturbed stream functions are also shown (solid where positive, dashed where negative; .05 Sv spacing).